To be presented at the   BNL - 45290
Third Annual 1991 International Industrial Symposium
on the Super Collider (IISSC)
Atlanta Hilton and Towers
Atlanta, Georgia
March 13-15, 1991

SSC 50 MM DIPOLE CROSS SECTION*

R.C. Gupta, S.A. Kahn and G.H. Morgan

Accelerator Development Department
Brookhaven National Laboratory
Upton, NY 11973 USA

Abstract

In this paper we present the magnetic design of the two dimensional coil and iron cross section, referred[1,2] to as DSX201/W6733, for the 50 mm aperture main ring dipole magnet for the Superconducting Super Collider (SSC). The computed values of the allowed field harmonics as a function of current, the quench performance predictions, the stored energy calculations, the effect of random errors on the coil placement and the Lorentz forces on the coil will be presented. The yoke has been optimized to reduce iron saturation effects on the field harmonics. We shall present the summary of this design which will include the expected overall performance of this cross section. Prototypes of these dipoles are being built at the Brookhaven National Laboratory (BNL) and at the Fermi National Accelerator Laboratory (FNAL). There are slight differences between the cross sections at the two laboratories.

Introduction

It has been decided to increase the aperture of the superconducting dipole magnet from 40 mm to 50 mm. In addition, it was recommended by the SSC 5 cm Dipole Task Force[3] to use wider cables than those used in the 4 cm dipole[4] to obtain a field margin of 10% over 6.6 tesla. However, due to a decrease in the effective magnetic length of the dipole, the design field for 20 TeV operation has been increased to 6.7 tesla. From beam dynamics considerations, this dipole is required to have smaller values of field harmonics and a smaller variation in them due to iron saturation than those originally specified for the SSC 4 cm dipole magnet.

The coil aperture in this magnet will actually be 49.56 mm instead of 50 mm. This reflects a slight change in the width of the cable used in the inner layer. Moreover, the thickness of the cable used in the outer layer was also changed. These modifications produce a small change in the values of field harmonics from their design value. An iteration in the basic coil design could be made to bring the harmonics back to their original values. However, due to various reasons the harmonics from the manufactured coil usually have a small systematic shift from those which the coil was designed to

_____

have. Therefore, to avoid delay in the magnet program, an iteration to obtain the desired harmonics in the production magnet could be incorporated after a few magnets are made.

The basic coil cross section in the BNL and FNAL magnets is the same except for a 10 mil difference in the pole angle of the outer layer. The differences in the iron cross section arise due to the fact that the BNL design has a horizontally split yoke, while the FNAL design has a vertically split yoke. These differences and their effect on the field quality will be discussed in more details in the following sections. However, in most respects, the two designs perform the same magnetically and unless otherwise mentioned, the following discussion applies to both.

Coil Design

The coil is made of two layers of superconducting cables. Some basic parameters of the cables used in the inner and outer layers are shown in Table 1. The cable used in the inner layer has 30 strands and in the outer layer 36.

Table 1: Cable properties of SSC 50 mm magnet with wider cables.

Cable parameters	Inner layer	Outer Layer
Filament diameter, micron	6.0	6.0
Strand diameter, mm	0.808	0.648
No. of strands	30	36
No. of strands × Strand Area, mm^2 (Approximate cable area)	15.382	11.872
Cable width, bare, mm	12.34	11.68
Cable width, insulated, mm	12.51	11.85
Cable mid-thickness, bare, mm	1.458	1.156
Cable mid-thickness, insulated, mm	1.626	1.331
Keystone, (max-min) thickness, mm	0.262	0.206

The coil is designed by placing the cables in such a way that they produce a field with a high degree of uniformity. This is done using the computer program PAR2DOPT[5] which uses analytic expressions for computing the field harmonics at the center of the magnet of coils in a circular $\infty\mu$ iron aperture. It also computes the peak field on the surface of the conductor.

We examined numerous configurations for the coil design. The one selected has a total of 45 turns in each quadrant in two layers. The inner layer has 19 turns in four blocks (three wedges) and the outer has 26 turns in two blocks (one wedge). During the coil optimization process, we closely monitored the peak field, i.e., the maximum value of magnetic field in the conductor, both in the inner and in the outer layer. For the same transfer function, a coil design with a lower peak field would produce a magnet which will quench at a higher current. In our search for the most optimum coil configuration, we kept the number of wedges in the outer layer to be one; however in the inner we looked for solutions with two or three wedges. The designs with two wedges in the inner layer were, in general, found to have a higher peak field or excessive harmonic content. For this reason, we chose a design having three wedges in the inner layer. The SSC 4 cm magnet also has three wedges in the inner layer and one in the outer. However, the present coil is optimized in such a way that the two wedges nearest to the pole in the inner layer are identical and symmetric. This design has performance comparable to those which did not have this imposition on the two wedges.

field harmonics in this magnet (However, it does not include the contributions from persistent currents in the superconductor). As mentioned earlier, for mechanical reasons, the size of the cable was changed by a small amount from the one assumed in the original design. This produces noteworthy deviations in the three lowest allowed field harmonics. The last row of the table, "Revised", refer to the values of field harmonics in the magnet after this change in the cable size.

Table 2: Desired and Optimized values of *low field* harmonics in prime units. The harmonics *in magnet* take into account the pole notch and a flat face in the iron at the midplane. These harmonics are in the units of 10^{-4}.

Values	b_2'	b_4'	b_6'	b_8'	b_{10}'	b_{12}'
Desired	-.28±.4	.01±.1	0±.05	±(.04to.05)	0±.05	0±.05
Optimized	-0.280	0.009	-0.004	0.044	0.014	-0.001
In BNL magnet	0.000	-0.001	-0.004	0.044	0.014	-0.001
Revised BNL	1.566	0.070	-0.024	0.043	0.015	-0.001
Revised FNAL	0.165	0.073	-0.021	0.043	0.015	-0.001

A small difference in the "Revised" BNL and FNAL harmonics is due to the fact that (a) the pole angle in the out layer of FNAL cross section is 10 mil smaller than in BNL and (b) the notch in the aperture of the vertically split iron is at the midplane and in the horizontally split iron is at the pole.

We have used the following definition for field harmonics

$$B_y + iB_x = B_0 \sum_{n=0}^{\infty} [b_n + ia_n][\cos(n\theta) + i \sin(n\theta)] \left(\frac{r}{R_0}\right)^n ,$$

where B_0 is the field at the center of the magnet, B_x and B_y the components of field at (r,θ), R_0 the normalization radius, a_n the skew harmonics and b_n the normal. These harmonics are usually quoted in prime units (b_n' and a_n') when R_0 is chosen to be 1 cm and the harmonics are given in 10^{-4} units.

Iron Yoke Design

In this section we shall discuss the process used in designing the iron yoke. The iron contributes about 22% to the magnetic field at 6.7 tesla (somewhat higher at lower field). Since the magnetization of the iron is not a linear function of current in the coil and since the magnetization of the iron is not the same throughout the cross section, the uniformity of the field becomes a function of the current in the coil. The yoke is optimized to produce a minimum change in field harmonics (due to iron saturation) for the maximum achievable value of transfer function at 6.7 tesla. We used computer codes POISSON, MDP and PE2D for this purpose. We shall compare the results of field computations done using these three codes. We shall discuss, in detail, the computer model of the final design and the results of field calculations for it with POISSON. An iron packing factor of 97.5% has been used in these calculations.

If no special technique for controlling iron saturation were used, the change in b_2' harmonic due to iron saturation will be over 1 unit. This is more than the desired change of less than 0.6 unit. The following three options were considered for reducing the b_2' saturation swing. They all try to control the iron saturation at the iron aperture so that it saturates evenly.

- Reduced (shaved) iron o.d.
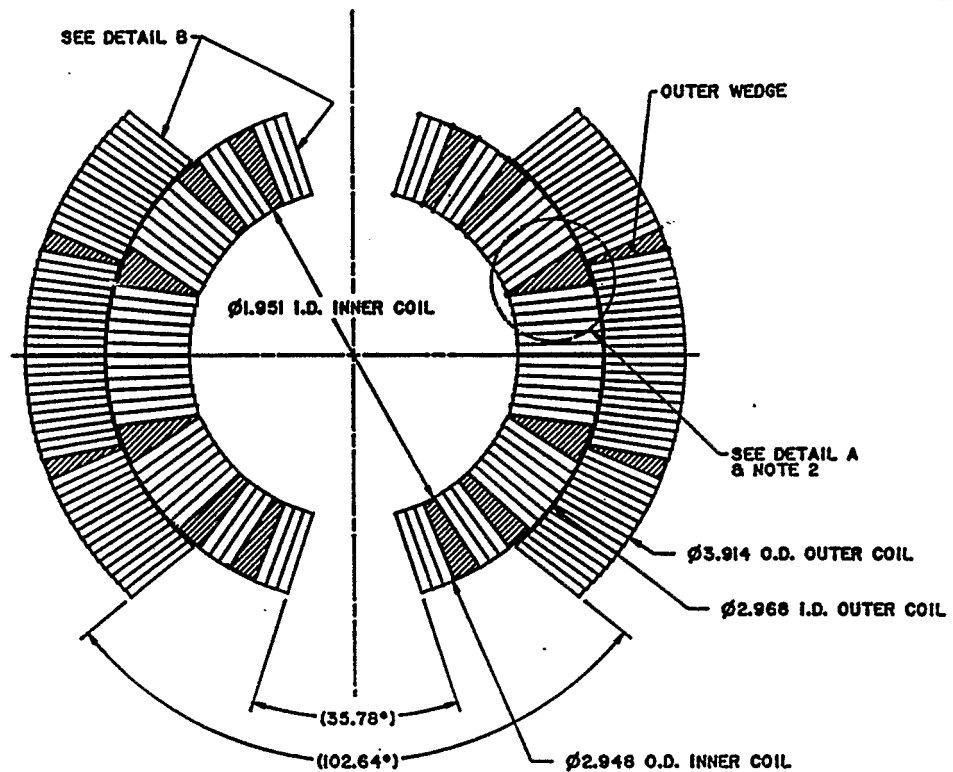
Figure 1: Optimized Coil for SSC 50 mm Dipole.

The physical layout of the optimized coil configuration is shown in Figure 1.

Low Field Harmonics

The iron aperture is not completely circular in this magnet. It has a pole notch and a small vertical straight face at the midplane. These structures introduce small but noticeable non-zero values of b_2' and b_4' harmonics. These harmonics should be cancelled out in a coil design if the magnet is to produce zero low field harmonics. Therefore, to cancel the effect of non-circular iron inner radius, -0.28 prime units of b_2' and +0.01 of b_4', were desired in the optimized coil. In addition, a non-zero value of b_8' harmonic was desired for centering the coil during the field measurements. Since the given tolerance in b_8' was 0.05 prime unit, we looked for a solution which had a magnitude of this harmonic between 0.04 and 0.05. This requirement on b_8' threw many designs out of running. However, the final design which satisfied all of above requirements was no worse in performance to those which did not.

In Table 2 we have given the desired and optimized values of field harmonics in prime units. Harmonics, higher than b_{12}', had an optimized value of < 0.001, as desired. In the row of desired harmonics, we have also listed the allowed systematic errors in them. *"In BNL magnet"* harmonics takes into account the pole notch and a flat face in the iron at the midplane. These would be the expected values of low

- Stainless Steel (non-magnetic) key at the midplane
- Shim at the iron inner surface

The first scheme, though most straight forward, produces a large loss in transfer function at 6.7 tesla than the other two schemes. The third scheme, though actually increasing the transfer function at 6.7 tesla due to extra iron, requires more engineering development due to its non-circular aperture. The second scheme produces very little loss in transfer function (0.3% at 6.7 tesla compared to a keyless or magnetic key version) for a comparatively large reduction in b_2' saturation ($\frac{3}{4}$ unit). Moreover, it also has the advantage of giving a lever (within limits) for controlling b_2' saturation by changing the location and/or size of the key without affecting the other parts of the magnet design. This is so because nothing changes at the iron inner or outer surface. If the measurements don't match with the calculations due to any reason, then this could be a very useful and convenient handle to empirically correct the b_2 versus I curve. In the past, measurements and calculations have agreed to a few tenth of prime unit when the change in b_2' harmonic due to iron saturation was compared. It may be pointed out that besides iron saturation, b_2 and other harmonics are also a function of current because of the coil deformation due to Lorentz forces.

The POISSON model of the optimized yoke for the horizontally split iron (BNL) is shown in Figure 2 and for the vertically split iron (FNAL) in Figure 3 which also shows the field lines at 6500 ampere. The iron i.d. is 5.339″. This leaves a space of 17 mm for the collar. The iron o.d. is 13.0″. This value is a slight reduction from the value $\left(13.22''\right)$ obtained by extrapolation of the present 4 cm aperture design, and hence includes a bit of iron shaving. The stainless steel key in the horizontally split yoke design is located at 3.6″ and has a size of $\frac{1}{4}''\times\frac{1}{4}''$. In the vertically split design a cutout at the midplane is incorporated to reduce the iron saturation. The size and location of this cutout is the same as in the BNL yoke where it was intended for the stainless steel key. As mentioned earlier, the iron aperture is not completely circular. The BNL yoke has a pole notch of size 0.201″ × 0.105″ and a vertical straight face at the midplane which starts at $x = 2.643''$. The FNAL yoke has both the notch and a vertical face at the midplane. The FNAL yoke has an additional pin located below the bus slot. This pin is made of non-magnetic steel and produces a noticeable effect on iron saturation. Other structures in the two yokes are shown in the above mentioned figures.

In Table 3, we list the transfer function (T.F.) and b_2' as a function of current as computed by POISSON, MDP and PE2D in the BNL yoke and by POISSON in the case of FNAL yoke. The low field b_2' harmonic has been corrected so that it starts from zero; a non-zero value is artificial and is related to the way the computer model of a given coil and iron geometry is set up in these three codes. The maximum b_2' saturation, as computed by the three codes is about 0.3 prime unit. Please note that the calculations presented in this paper do not include the effect of the cryostat wall. POISSON uses a generalized finite difference method, MDP uses an integral method and PE2D uses the finite element method. Despite the fact that these three programs uses three different methods for solving the problem, it is encouraging to see that all predict a small saturation shift.
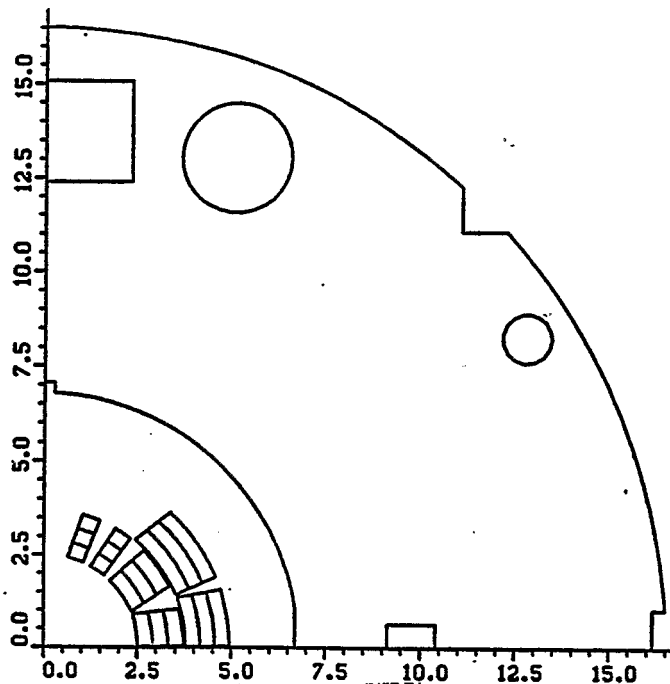
Figure 2: POISSON model for SSC 50 mm Dipole with the horizontally split iron lamination.
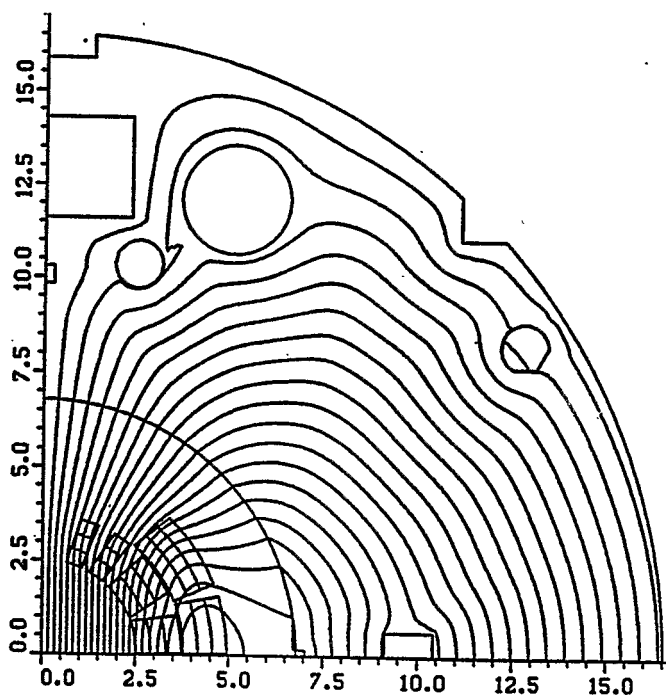
Figure 3: POISSON model and field lines at 6500 ampere for SSC 50 mm Dipole with the vertically split iron lamination.

Table 3: Transfer function and b'_2 variation as function of current. In all cases b'_2 is corrected to start from zero at 3.0 kA.

I	T.F. (T/kA)				$b'_2 \times 10^{-4}$			
kA	FNAL	POISSON	MDP	PE2D	FNAL	POISSON	MDP	PE2D
	yoke	BNL yoke			yoke	BNL yoke		
3.0	1.0450	1.0447	1.0430	1.0430	0.00	0.00	0.00	0.00
4.0	1.0445	1.0441	1.0413	1.0423	-0.02	0.08	0.05	0.12
5.0	1.0398	1.0397	1.0364	1.0374	-0.04	0.22	0.16	0.24
5.5	1.0339	1.0340	1.0311	1.0318	0.19	0.26	0.21	0.27
6.0	1.0257	1.0262	1.0236	1.0243	0.36	0.14	0.17	0.28
6.25	1.0209	1.0219	1.0194	1.0201	0.38	0.07	0.11	0.26
6.5	1.0159	1.0173	1.0148	1.0156	0.35	-0.03	0.03	0.22
7.0	1.0053	1.0073	1.0051	1.0066	0.17	-0.33	-0.19	0.10
7.6	0.9926	0.9955	0.9935	0.9956	-0.15	-0.77	-0.60	-0.07
8.0	0.9845	0.9877	0.9861	0.9890	-0.38	-1.06	-0.85	-0.22
8.6	0.9732	0.9766	0.9758	0.9789	-0.70	-1.43	-1.20	-0.43

In Table 4 we have listed the maximum change in b'_2 and b'_4 harmonics due to iron saturation as computed by these codes. All other higher harmonics remain practically unchanged. In the same table we have also listed the drop in transfer function, $\delta(TF)$, at 6.6 tesla as compared to its value at low field. In the case of the FNAL yoke, the computations have been done only with the code POISSON.

Table 4: Drop in transfer function at 6.6 tesla and the maximum change in b'_2 and b_4'; higher harmonics remain practically unchanged.

Harmonic	POISSON FNAL yoke	POISSON BNL yoke	MDP BNL yoke	PE2D BNL yoke
$\delta(TF)$, at 6.6T	2.84%	2.62%	2.70%	2.63 %
$\delta\left(b'_2\right)_{max}$, 10^{-4}	0.36	0.28	0.22	0.36
$\delta\left(b'_4\right)_{max}$, 10^{-4}	0.02	-0.03	-0.02	-0.04

In Table 5 we present the results of POISSON calculations for various values of current per turn in BNL yoke. In Figure 4, we plot the variation of field harmonics as a function of central field.

Table 5: Results of POISSON computations for SSC 50 mm Dipole for the horizontally split yoke design being built at BNL.

I kA	B_0 tesla	T.F. T/kA	b'_2 10^{-4}	b'_4 10^{-4}	b'_6 10^{-4}	b'_8 10^{-4}	b'_{10} 10^{-4}	b'_{12} 10^{-4}
$\infty\mu$	$\infty\mu$	1.04493	0.020	-0.046	0.000	0.047	0.015	-0.001
3.000	3.1341	1.04471	0.031	-0.046	0.001	0.047	0.015	-0.001
4.000	4.1762	1.04406	0.111	-0.050	0.001	0.047	0.015	-0.001
4.500	4.6921	1.04268	0.140	-0.055	0.001	0.047	0.015	-0.001
4.750	4.9464	1.04135	0.182	-0.060	0.001	0.047	0.015	-0.001
5.000	5.1985	1.03969	0.255	-0.063	0.001	0.047	0.015	-0.001
5.250	5.4454	1.03721	0.299	-0.066	0.001	0.047	0.015	-0.001
5.500	5.6871	1.03402	0.291	-0.069	0.001	0.048	0.015	-0.001
5.750	5.9240	1.03027	0.235	-0.071	0.001	0.048	0.015	-0.001
6.000	6.1573	1.02621	0.172	-0.073	0.000	0.048	0.015	-0.001
6.250	6.3868	1.02189	0.100	-0.073	0.000	0.048	0.015	-0.001
6.500	6.6121	1.01725	-0.003	-0.072	0.000	0.048	0.015	-0.001
7.000	7.0513	1.00733	-0.300	-0.072	0.000	0.049	0.015	-0.001
7.500	7.5654	0.99545	-0.738	-0.070	0.000	0.049	0.015	-0.001
8.000	7.9014	0.98767	-1.032	-0.068	0.000	0.050	0.015	-0.001
8.500	8.3984	0.97656	-1.403	-0.064	0.000	0.050	0.015	-0.001
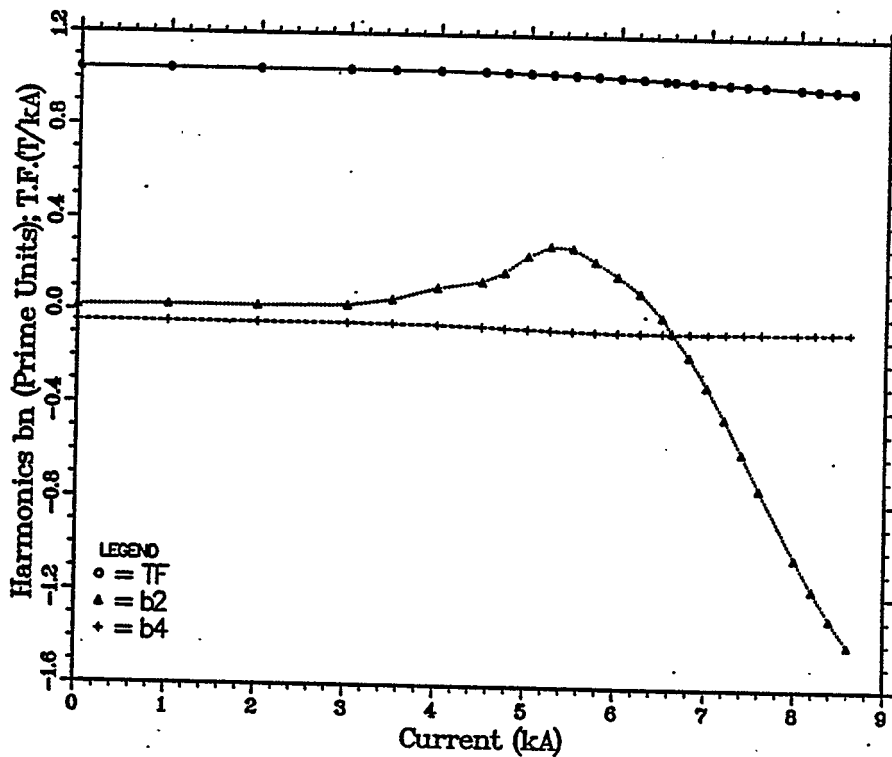
Figure 4: Variation in Field Harmonics as a function of Current for SSC 50 mm magnet as computed by POISSON.

Expected Quench Performance

The central field at which the cable looses its superconducting properties (B_{ss}, with "ss" standing for Short Sample) depends[5,6] on the maximum magnetic field in the conductor (peak field), the bath temperature, the current density in the cable and the quality of the cable itself (degradation). We have listed the peak field (B_{pk}) in the inner and outer layers in Table 6 for two values of central field (B_o). The ratio of B_{pk} to B_o, the *Enhancement Factor*, is given in the next column. In each layer, the peak field is found on the upper edge of the top (pole) most turn. The location of it is expressed in % of the cable width as measured from the upper-left corner of that turn. In the next column we list this location. We have done the peak field calculations using the code MDP which is considered to be better suited to this purpose.

Table 6: Peak fields in SSC 50 mm Dipole as computed with MDP.

I	B_o	Inner			Outer		
kA	tesla	B_{pk},T	$\frac{B_{pk}}{B_o}$	Location	B_{pk},T	$\frac{B_{pk}}{B_o}$	Location
6.85	6.9058	7.2374	1.048	5%	6.0016	0.869	11%
7.20	7.2100	7.5595	1.048	5%	6.2660	0.869	11%

Our calculations assume that the superconducting wire will have a critical current density $J_c(5T, 4.2K)$ of 2750 amp/mm^2. The quality of the superconductor gets degraded when the cable is made out of these wires and put in the magnet. We have done calculations with 5% degradation (J_c=2612.5) in Table 7 at 4.35° kelvin bath temperature.

Table 7: Expected quench performance of SSC 50 mm Dipole with 5% cable degradation ($J_c = 2612.5 Amp/mm^2$) and at 4.35° kelvin temperature.

Layer ↓	Cu/Sc Ratio	B_{ss} tesla	I_c amp	B_{margin} %over 6.7T	T_{margin} kelvin	S_{quench} amp/cm²	$S_{6.7T}$ amp/cm²
Inner	1.7	7.149	7126	6.7	0.519	736	681
	1.5	7.273	7273	8.6	0.625	788	715
	1.3	7.399	7411	10.4	0.730	853	759
Outer	2.0	7.268	7267	8.7	0.580	919	834
	1.8	7.445	7470	11.1	0.709	980	865

In these tables we have listed the Field Margin (B_{margin}) and the Temperature Margin (T_{margin}). The temperature margin is defined as the maximum possible computed rise in the operating temperature (over the design value of normal operation, which is 4.35° K) before which the magnet will quench at the design central field (B_{design}=6.5 tesla). The Field Margin is defined as follows

$$B_{margin}(\%) = \frac{B_{ss} - B_{design}}{B_{design}} \times 100$$

In the outer layer a copper to superconductor ratio, CSR or Cu/Sc, of 2.0 and 1.8 is used in the calculations. In the inner layer we have done these calculations for Cu/Sc ratios of 1.7, 1.5 and 1.3. We have listed the computed central field (B_{ss}) when the magnet is expected to quench, the current in the cable at that time (I_c) and the current density (S_{quench}) in copper to carry that current. A lower current density in copper is expected to give a better stability. We have also given the current density in the copper at 6.7 tesla ($S_{6.7T}$). When comparing the two cases in a table, $S_{6.7T}$ is a more appropriate parameter to consider than S_{quench}.

The design estimates of quench field, etc., have been listed in Table 7. They presume a degradation of 5% (J_c=2612.5), bath temperature of 4.35° kelvin and a copper to superconductor ratio of 1.8 in the outer layer and of 1.5 in the inner layer. The quench field of 7.273 tesla in the inner layer gives a field margin of 8.6% over the design operating field of 6.7 tesla. The quench field of 7.445 tesla in the outer layer gives a field margin of 11.1%.

Estimating the Effect of Random Errors

Due to various reasons the actual value of a parameter used in designing the coil may come out to be some what different than desired. In particular, we are interested in variations in the locations of the turns in the coil. This causes a change in the transfer function and field harmonics. In this section the effect of these errors in various cases are estimated using the procedure developed by P.A. Thompson[7]. The basic four fold symmetry in the dipole coil geometry is retained in this analysis. Though this is not a realistic assumption, it is useful in estimating the size of some random errors. In Table 8 these effects are listed for a nominal 0.05 mm variation in the given parameter.

Table 8: The effect of 0.05 mm change in the given parameter on the transfer function and the field harmonics.

Parameter changed	TF T/kA	b_2' 10^{-4}	b_4' 10^{-4}	b_6' 10^{-4}
Block No. 1	0.31	-0.25	-0.10	-0.01
Block No. 2	-0.32	0.31	0.12	0.01
Block No. 3	-0.12	0.36	-0.02	-0.01
Block No. 4	-0.20	0.33	-0.08	0.01
Block No. 5	-0.11	-0.04	-0.01	0.00
Block No. 6	-0.78	0.22	0.03	0.00
RMS Blocks	0.38	0.27	0.07	0.01
Wedge No. 1	-1.56	-0.48	0.02	0.01
Wedge No. 2	0.83	0.59	0.05	-0.01
Wedge No. 3	2.32	0.71	-0.04	0.00
Wedge No. 4	-0.57	-0.11	0.00	0.00
RMS Wedges	1.48	0.52	0.03	0.01
Cable thickness inner	2.63	1.08	0.05	-0.01
Cable thickness outer	1.99	0.48	0.02	0.00
RMS Cable thickness	2.33	0.83	0.04	0.01
Pole angle inner	-4.01	-0.45	0.06	-0.01
Pole angle outer	-2.26	-0.42	0.00	0.00
RMS Pole angles	3.25	0.43	0.04	0.01

First we have given the effect of changing the radius of every turn in each current block by +0.05 mm. The counting of the blocks in the table is done by starting from the inner layer and from the midplane of each layer. Next we estimate the effect of changing the wedge size by +0.05 mm. Pole angle is held constant in this calculation by reducing the conductor thickness by an appropriate amount. The counting scheme for the wedges is the same as it was for the current blocks. It is possible that during the molding, the thickness of the cable does not get reduced uniformly within a layer. To estimate this effect, a linear change in the cable thickness is assumed in going from

the midplane to pole such that the middle turn is displaced azimuthally by 0.05 mm. The pole angle does not change during this perturbation. This effect is given for the inner and outer layers in the next two rows of this table. We also estimate the effect of increasing the pole angle by 0.05 mm in the inner and in the outer layer. We also compute the Root Mean Square (RMS) change for each group of these variations.

Stored Energy and Inductance Calculations

We have done stored energy calculations with the computer codes POISSON and PE2D at 6.5 kA (6.6 tesla). The results are given in Table 9. In this table we have given the stored energy and inductance per unit length and for a 15 m long dipole. The inductance has been computed using the relation

$$Stored\ Energy = \tfrac{1}{2} Inductance \times (Current)^2.$$

Table 9: Stored Energy and Inductance calculations at 6.5 kA.

	POISSON	PE2D
Stored Energy per unit length, kJ/m	105.0	105.3
Stored Energy for 15 m long Dipole, kJ	1575.6	1579.8
Inductance per unit length, mH/m	4.972	4.986
Inductance for 15 m long Dipole, mH	74.585	74.783

Lorentz Force Calculations

The value of Lorentz force on each turn is obtained from the components of the magnetic field (B_x, B_y) which are calculated using the program MDP. However, B_x and B_y are not uniform in a turn. We obtain the average values of these components from a grid of 10 × 2 across the width and thickness of the cable.

The variation in the magnitude of the radial and azimuthal components of the Lorentz force, namely F_r and F_θ, with the turn number is shown in Figure 5. The turn numbers are counted from the midplane. The Lorentz force acts on the coil such that the azimuthal component compresses the coil on the midplane and the radial component expands it outward. Though the radial force on the turns in the outer layer is very small, the force on the turns in the inner layer must be transmitted through the outer layer to the structure of the magnet. In Figure 6 we have shown the direction and magnitude of the total force in each block. The arrows represent the size and the magnitude of the force. Please note that the force in a block is a vector sum of the force acting on the individual turns of that block.
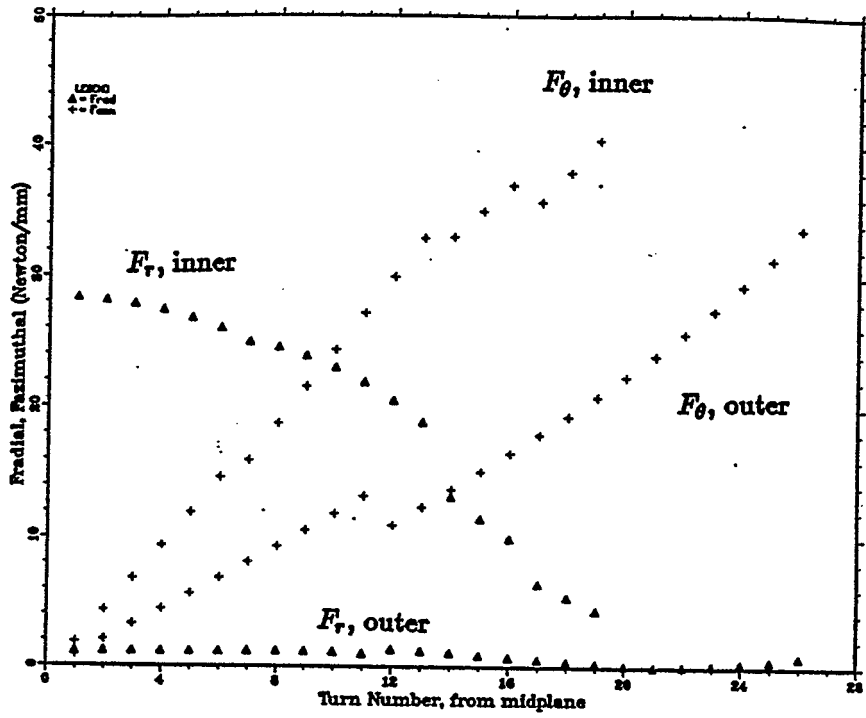
Figure 5: Magnitude of the Lorentz Force on each turn.
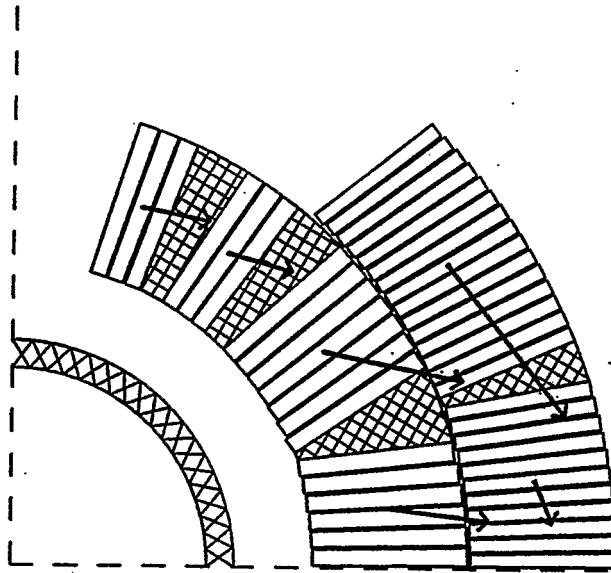
Figure 6: Lorentz Force on each block.

Summary of the Design

In this section we present the summary of this design. It includes various dimensions and the expected performance of this cross section. The summary of the coil cross section is given in Table 10. The coil has two layers and the number of turns are the number of turns in each quadrant in a layer. The field margin in this cross section is limited by the inner layer. If the cable used in the inner layer has a copper to superconductor ratio of 1.3, the margin would be 10.4%. The summary of the iron cross section and the effect of saturation on field harmonics is given in Table 11.

Table 10: Summary of SSC 50 mm Dipole Coil Cross section.

Layer →	Inner	Outer
No. of Turns	19	26
Strand Diameter, mm	0.808	0.648
Strands per turn	30	36
Coil i.d., mm	49.56	74.91
Coil o.d., mm	75.36	99.42
B_{peak}/B_o Ratio	1.048	0.869
Cu/Sc Ratio	1.5	1.8
Margin over 6.7 T ...	8.6%	11.1%

Table 11: Summary of SSC 50 mm Dipole Iron Cross section.

Inner Diameter, mm	135.6
Outer Diameter, mm	330.2
$\delta(TF)$, till 6.7 T	2.6%
δb_2, prime unit	0.3
δb_4, prime unit	0.03

References

1. R.C. Gupta, S.A. Kahn, G.H. Morgan, "DSX201/W6733 - Coil and Iron Design for SSC 50 mm Dipole Magnet with Wider Cable", SSC Technical Note No. 88 (SSCL-N-699), June 28,1990.

2. R.C. Gupta, "Magnetic Properties of Fermilab 50 mm Aperture Dipole for Superconducting Super Collider", Magnet Division (internal) Note No. 361-1(SSC-MD-254), September 12, 1990.

3. SSC 50 mm Dipole Task Force headed by R. Palmer (3/90).

4. SSC Conceptual Design Report, SSC-SR-2020, March 1986.

5. G. Morgan, "SSC Reference Design Dipole", Magnet Division (internal) Note No. 53-1, March 12, 1984.

6. G. Morgan, "New Coefficients for a $J_c(B,T)$ Analytic Form", SSC Technical Note No. 76 (SSC-N-519), June 10,1988.

7. PAR2DOPT is an analytic coil design program which is presently maintained and developed by P. Thompson. This is a modified version of a program which was mostly written earlier by R. Fernow and later in part by G. Morgan.